ACS APPLIED MATERIALS & INTERFACES

Research Article

www.acsami.org

Mesoporous Organosilica Nanoparticles Containing Superacid and Click Functionalities Leading to Cooperativity in Biocidal Coatings

Julia Gehring,[†] David Schleheck,[‡] Bastian Trepka,[†] and Sebastian Polarz*,[†]

[†]Department of Chemistry and [‡]Department of Biology, University of Konstanz, D-78457 Konstanz, Germany

Supporting Information

ABSTRACT: A superior degree of functionality in materials can be expected, if two or more operational entities are related in a cooperative form. It is obvious that, for this purpose, one is seeking materials with complex design comprising bi- or multiple functional groups complementing each other. In the current paper, it is demonstrated that periodically ordered mesoporous organosilicas (PMOs) based on co-condensation of sol–gel precursors with bridging phenyl derivatives $R_{F1,2}C_6H_3[Si(O^{iso}Pr)_3]_2$ allow for rich opportunities in providing high-surface area materials with such a special chemical architecture. PMOs containing high density of thiol ($\cong R_{F1}$) and sulfonic acid units ($\cong R_{F2}$) were prepared as mesoporous nanoparticles via an aerosol-assisted gas-phase method and were tested for biocidal applications. Each of the mentioned organic groups fulfills several tasks at once. The selective functionalization of thiols located at the surface of the particles using click chemistry leads to durable grafting on different substrates like glass or stainless steel, and the intraparticle −SH groups are important regarding the uptake of metal ions like Ag^+ and for immobilization of Ag^0 nanoparticles inside the pores as an enduring reservoir for antibacterial force. The superacidic sulfonic acid groups exhibit a strong and instantaneous biocidal acitivity, and they are important for adjusting the Ag^+ release rate. Biological studies involving inhibitory investigation tests (MIC), fluorescence microscopy (life/dead staining), and bacterial adhesion tests with *Pseudomonas aeruginosa* show that the organobifunctional materials present much better performance against biofilm formation compared to materials containing only one of the above-mentioned groups.

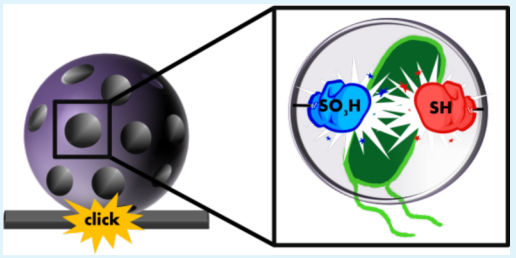

KEYWORDS: *mesoporous particles, multifunctional materials, surface immobilization, antifouling, click chemistry*

INTRODUCTION

Surface colonization and biofouling is a significant problem in almost every area where wet surfaces stay in contact with micro-organisms. Examples are medical devices, biosensors, and the food and shipping industry, to name only a few.[1,2] Due to the negative effects of microorganism accumulation and their byproducts on surfaces, preventing biofilm formation is an important issue and has attracted great attention.[3,4] Biofouling starts with nonspecific adsorption of cells and their biomolecules on surfaces, leading to initial colonization, and after cell proliferation ends up with highly stable networks of microorganisms embedded in extracellular polymeric substances (slime). Different approaches for biofouling prevention have been described in the literature.[1] One can differentiate between two general strategies: either preventing the initial cell attachment and formation of biofilms or degrading and removing pre-established biofilms.

A key approach for protecting surfaces against fouling processes is the use of biocidal agents. Whereas antibiotics are very powerful, their disadvantage is not only the fast development of resistances, but regarding surface protection they are also less suitable because of their high price, fast leaching, and the resulting short effective period. As an alternative, silver cations (Ag^+) act as an electron donor blocker, can deactivate biological groups containing oxygen, sulfur, or nitrogen, and inhibit the respiratory process in cells.[5] Thus, silver nanoparticles represent one of the most popular antifouling materials these days.[6] They are commonly applied in wound dressings, catheters,[7] and textiles.[8] Free, respectively, dissolved Ag^+ originates from oxidative processes in aqueous media (e.g., caused by dissolved oxygen), and therefore silver nanoparticles have been recognized to serve as a permanent silver ion source. The mentioned oxidation processes take place on the particle surface, which explains the fact that nanoparticles ranging from 2 to 10 nm show the strongest biocidal effect due to their high surface area.[9] However, silver nanoparticles are also discussed controversially because of the risk for the undesired penetration into the human body, where they can be harmful.[10] Hence, immobilizing silver nanoparticles on surfaces becomes necessary. Embedding silver nanoparticles into polymers,[11,12] fiber glasses, or hydrogels or immobilization on materials like silica[13] or carbon nanotubes[14] supports the prevention of exposure to the environment and improves the silver ion release control.[15]

Mesoporous silica materials also possess a great potential for hosting silver nanoparticles by offering a well accessible pore

Received: November 26, 2014
Accepted: December 15, 2014
Published: December 15, 2014

DOI: 10.1021/am5083057
ACS Appl. Mater. Interfaces 2015, 7, 1021−1029

system and a large internal surface area up to 1000 m^2/g.[16,17] Either premade Ag nanoparticles are infiltrated into the pore system or Ag^+ salts are used, followed by reduction with agents like $NaBH_4$,[18] glucose,[19] hydrogen,[13] or ascorbic acid.[20] The great advantage of the latter approach is the direct synthesis of silver nanoparticles inside the pores[13] leading to nonblocked pore entrances and a homogeneous distribution of silver nanoparticles. Both factors favor the control of biocidal activity[21] as well as the stability of the nanometer-sized silver nanoparticles.[22] A further advantage of using nanoporous silica materials is the possibility to prepare hybrid materials equipped with a wide range of organic functional groups.[23,24] A nice example demonstrating the relevance of functional groups at the surfaces was published by Wang and co-workers, who modified mesoporous silica materials using (3-mercaptopropyl)-trimethoxysilane. It was seen that the use of organic thiols facilitates the adsorption of silver nanoparticles on the surface.[25]

Organically modified, mesoporous silica materials can be obtained via different methods. The so-called grafting (respectively, postmodification) and co-condensation routes are popular functionalization methods, also because a range of organically modified alkoxysilane precursors are commercially available.[26] However, the major disadvantage of the latter two methods is that the modification degree (max. 25%) is typically relatively low. Only very recently high organic content organosilica materials could be obtained via co-condensation.[27] For some applications, a higher degree of organic modification is preferred, and in these cases the so-called PMO (periodically ordered mesoporous organosilica) approach seems to be more suitable. Porous materials with 100% degree in organic modification can be prepared using special sol−gel precursors containing bridging organic groups, $((R'O)_3Si-R-Si(OR')_3)$.[28−32] The reader interested in an overview of the PMO field is referred to one of the recent review articles.[33−35] In our laboratory we developed the UKON-PMO system for designing porous materials with tailor-made surface properties.[36−44] All UKON materials are based on special sol−gel precursors with a bridging phenyl entity modified with several functional groups R_F in the 3-position of the aromatic ring. Recently we described a PMO material containing benzenesulfonic acid functionalities, its superacidic properties, and its antibacterial properties.[44] However, whereas the biocidal property is very pronounced in the beginning, it drops as soon as the proton reservoir of the particles is used up.

Therefore, in the current contribution we introduce the concept that two different biocidal factors operate in one material system. They should not act independent of each other but with a certain degree of cooperativity if desired. For this purpose novel organosilica materials are prepared containing two different functional groups $R-SO_3H$ and R−SH. In general, there exist only few examples of materials comprising two different functional entities, which are geared to each other, respectively, and exhibit cooperative effects with each other. In the current case, we expect that each of the functional groups could exhibit two functions. The sulfonic acid will act as the first attack against the bacteria,[44] but it could, due to the locally enhanced acid environment inside the pores, also influence the dissolution of Ag and consequently the release of Ag^+ ($2Ag^0 + 2H^+ \rightarrow 2Ag^+ + H_2$). The thiol group is expected to interact with the silver species inside the pores, and it will be facilitated for the immobilization of nano-/microsized PMO particles on relevant surfaces like glass, polymers, or metals. The described goals will be reached by realizing the following steps

- Establishing novel PMO materials with thiol groups.
- Preparation of bifunctional mesoporous particles containing thiol and sulfonic acid groups.
- Preparation of Ag nanoparticles inside the mesoporous, bifunctional PMO particles.
- Immobilization of the resulting particles on solid surfaces.
- Biological tests for their antibacterial activity.

EXPERIMENTAL SECTION

Materials. Chemicals were received from Sigma-Aldrich, and prior to use they were carefully purified and dried, when applicable. Glass slides were purchased from Marienfeld; 15 × 15 mm. Using the Schlenk technique all reactions on the precursor state were performed under inert conditions. The syntheses of 1,3-bistri(isopropoxy)silyl-5-bromobenze and 3,5-bistri(isopropoxy)silylbenzene-3-sulfonyl chloride have been described previously. For UV irradiation we used a handlamp (Peschl ultraviolet; 250 W) model SwiftCure HL-250. Silver ion detection was performed by a silver ion selective electrode (Cole Parmer combination ion selective electrode Ag^+/S^{2-}).

Synthesis of 1,5-Bistri(isopropoxysilyl)-benzene-3-thiol (3). To a solution of 1.5 g of 1,3-bistri(isopropoxy)silyl-5-bromobenze (2.65 mmol) in 50 mL of dry Et_2O was added ^{t}BuLi (3.5 mL, 1.5 M, 5.3 mmol) dropwise at −78 °C. The mixture was stirred for 30 min. Then 85 mg of S_8 (2.65 mmol) was added and stirred for another 30 min at −78 °C. Afterward the colorless solution was warmed to room temperature and stirred for 1.5 h. Then the reaction was hydrolyzed with 30 mL of dry isopropanol. After removal of the solvent a yellow oil can be obtained. For further purification column chromatography was applied (silica gel 60; CH_2Cl_2/pentane 2/1). Finally 0.65 g (1.25 mmol; 47%) of a colorless oil was obtained. ^{1}H NMR (400 MHz, $CDCl_3$): δ/[ppm] 1.21 (d, 36H, ^3J = 6.1 Hz, ^{i}Pr-CH_3); 3.45 (s, 1H, SH); 4.24 (sept, 6H, ^3J = 6.1 Hz, ^{i}Pr-CH); 7.62 (m, 2H, o-arom. H); 7.77 (m, 1H, p-arom. H). ^{13}C NMR (100.61 MHz, $CDCl_3$): δ/[ppm] 25.6 (^{i}Pr-CH_3); 65.6 (^{i}Pr-CH); 129.7 (C-SH); 133.5 (Si-arom. C); 137.4 (p-arom. C); 138.7 (o-arom. C).

Preparation of UKON-2j under pH Control Using Buffer Systems. A total of 0.4 g of precursor (**3**) and 280 mg of pluronic F127 were dissolved in 1.6 g of buffer solution (pH 1.9). The mixture was prehydrolyzed for 3 h at 60 °C and aged for 7 days at room temperature. Afterward the resulting monolithic pieces were dried at 100 °C for 24 h. The template was removed by liquid extraction with 25 mL of ethanol and 25 mL of HCl (conc.) at 60 °C within 2−4 days.

Preparation of Bifunctional PMOs Containing Thiol and Sulfonic Acid Groups. The materials were prepared similar to the method described for UKON-2j. However, after prehydrolyzing the precursors separately (for precursor (**2**) 1 h and precursor (**3**) 3 h) the solutions were combined and aged for 4 days. Different ratios of the sol−gel precursors 1,5-bistri(isopropoxysilyl)-benzene-3-sulfonyl chloride and 1,5-bistri(isopropoxysilyl)-benzene-3-thiol were used. Pluronic P123 (for a 0.5 mmol precursor mixture 260 mg of P123 is used) as well as pluronic F127 are applied as structure-directing agents. The composition of the resulting, mesoporous organosilica materials can be described as UKON $(SH-PhSi_2O_3)1-x(SO_3H-PhSi_2O_3)x$.

Aerosol Synthesis of Mesoporous UKON-2j. An amount of 2.66 g (5.1 mmol) of 1,5-bistri(isopropoxysilyl)-benzene-3-thiol (**3**) was dissolved in 3.35 g of ethanol, and 0.18 g of H_2O and 2 μL of HCl (1 M) were added dropwise (pH 5.0) and refluxed for 18 h at 60 °C. The sol was diluted with 5 g of buffer solution at pH 1.9 (EtOH:H_2O; 4:1) and 0.6 g of pluronic P123 as surfactant (pH 3). The final reactant mole ratios (prec: EtOH:H_2O:P123) were 1:44:10:0.0224. The spherical mesoporous nanoparticles were obtained using an aerosol reactor (TSI Inc., model 3076) at a volumetric flow rate of 1.7 L min^{-1}. The aerosol was heated to 400 °C for 6.2 s and finally collected on a PTFE filter (average pore size 450 nm). Template removal was performed by liquid extraction with 15 mL of EtOH and 15 mL of HCl conc. at 60 °C for 4 days. Full characterization occurred

DOI: 10.1021/am5083057
ACS Appl. Mater. Interfaces 2015, 7, 1021−1029

via IR, TEM, SAXS, N_2 physisorption, and solid-state NMR (see Supporting Information (SI)).

Aerosol Synthesis of Bifunctional Mesoporous Nanoparticles Containing Thiol and Sulfonic Acid Groups. The materials were prepared similar to the method described for UKON-2j nanoparticles. However, different ratios of the sol−gel precursors 1,5-bistri(isopropoxysilyl)-benzene-3-sulfonyl chloride (**2**) and 1,5-bistri(isopropoxysilyl)-benzene-3-thiol (**3**) were used. The prehydrolysis step was performed separately. The UKON precursor (**2**) was prehydrolyzed for 5 h and the precursor (**3**) for 18 h at 60 °C. The sol was diluted with buffer solution (pH 1.9) and 0.6 g of pluronic P123 followed by tetrabutylammonium chloride (pH 3.1). The final reactant mole ratios (prec: $EtOH:H_2O:P123:Bu_4NCl$) were 1:44:10:0.0224:0.25. The aerosol synthesis including the parameters, volumetric flow rate of 1.7 L min^{-1}, 400 °C heating temperature, and heating time of 6.2 s, was performed as described for UKON-2j as well as the liquid extraction method. The composition of the resulting, mesoporous organosilica nanoparticles can be described as UKON $(SH\text{-}PhSi_2O_3)_1{-}x(SO_3H\text{-}PhSi_2O_3)x$.

Silver Nanoparticle Synthesis on UKON PMO Materials and PMO Nanoparticles. An amount of 0.2 mmol of UKON PMO materials or UKON PMO nanoparticles was stirred in 4 mL of aqueous $AgNO_3$ solution (0.1 M) at room temperature for 4 h. Afterward the materials were intensively washed with 20 mL of H_2O to remove noncoordinated silver ions. Then the Ag^+@UKON materials were suspended in 70 mL of H_2O dest., and 4 mL of a freshly prepared solution of ascorbic acid (0.005 M) was added dropwise. After 30 min the reaction was completed. The Ag^0@UKON PMO materials/Ag^0@UKON PMO nanoparticle were centrifugated and washed with 50 mL of H_2O dest.

Preparation of UKON Nanoparticle Coating on Glass. First commercial glass slides were activated by dipping them into a piranha solution (H_2SO_4:H_2O_2; 2:1 v/v) for 1 h at room temperature. Then the glass slides were rinsed with distilled water and dried at 80 °C for 4 h. To a 50 vol % solution of allyltrimethoxysilane and dry THF was added 0.4 vol % HCl conc. The silane-containing solution was spin coated on the glass slide with a speed of 20 rps and then baked at 150 °C for 3 h. Sequential washing with CH_2Cl_2, hexane, and acetone was performed afterward. Finally the glass slides were dried at 80 °C for 1 h. For the nanoparticle coating the as-prepared glass slides were placed in a suspension of UKON nanoparticles (10 w %) in isopropanol. Then the solvent was removed at 60 °C under atmospheric pressure. Afterward the glass slides were dried at 80 °C for 2 h. For detailed characterization see the Supporting Information.

Preparation of UKON Nanoparticle Coating on Stainless Steel. According to the procedure above commercially available stainless steel plates have been modified and coated with UKON PMO nanoparticles. Characterization of the coated plates is given in the Supporting Information.

Immobilization of UKON Nanoparticles on Glass via Click Chemistry. For the click reaction the coated glass slides were irradiated for 1 h at 365 nm without further treatments. For testing the stability of the coating the glass slides were shaken in H_2O dest. for 3 days at 250 rpm. SEM investigations before and after the shaking process were made.

Silver Nanoparticle Synthesis on UKON Nanoparticles Covalently Bound to Glass Surfaces. The materials were prepared according to the method described below. However, the particle-coated glass slides were put into 1 mL of aqueous $AgNO_3$ solution (0.1 M) at room temperature for 4 h and then washed with H_2O dest. Finally the slides were transferred into 5 mL of H_2O dest. and shaken at 70 rpm. An amount of 0.3 mL of ascorbic acid (0.005 M) was added dropwise. The reaction mixture was shaken for 30 min at 70 rpm, washed with H_2O dest., and dried in air.

Minimum Inhibitory Concentration (MIC) for UKON np@Ag. Amounts of 2 mL of aqueous Ag^0@UKON PMO nanoparticle solution with different concentrations (1, 0.75, 0.5, 0.25, and 1 mg/mL) were added to 2 mL of bacteria suspensions of *Pseudomonas aeruginosa* (concentrations 5 × 10^9 CFU/mL). The mixture was incubated at 37 °C for 24 h with shaking speed of 200 rpm. The turbidities of bacteria were observed after 24 h, and the minimal concentration of Ag^0@UKON PMO nanoparticle in the tube remaining clear is MIC. The MIC experiment was performed with Ag^0@SH50 PMO nanoparticle and Ag^0@SH100 PMO nanoparticle.

Bacterial Survival Test. The prepared Ag^0@UKON PMO nanoparticle films on microscope glass slides, as well as pure, uncoated glass slides, were sterilized via UV irradiation for 15 min. Then, a 20 μL portion of *Pseudomonas aeruginosa* PAO1 cell suspension (app. 5 ×10^9 CFU/mL) was placed on each film. After incubation for 2 h at room temperature and rinsing with 1 mL of sterile H_2O, the slides were placed on nutrient agar plates (LB medium) with the bacterial contamination side down for a further 30 min. Then the slides were removed and the agar dishes incubated for 18 h at 30 °C and evaluated for formation of a homogeneous bacterial lawn in dependence of the surface coating used.

Live/Dead Staining and Fluorescence Microscopy. Ag^0@UKON PMO nanoparticle films on microscope glass slides were sterilized by UV irradiation and then "contaminated" (inoculated) with *Pseudomonas aeruginosa* as described above. Live/dead staining of attached bacteria was done following the manufacturer's instructions (LIVE/DEAD BacLight Bacterial Viability Kit for microscopy, Life Technologies), and the stained cells were visualized under a flourescence microscope equipped with the appropriate filter sets.

RESULTS AND DISCUSSION

Establishing Novel PMO Materials with Thiol Groups. The first, planned step involves the synthesis of the novel UKON PMO material containing thiophenol as a bridging organic function (UKON-2j). For this purpose the corresponding sol−gel precursor 1,3-bistri(isopropoxysilyl)-thiophenol (**3**) is required. Starting from compound (**1**) with bromobenzene as a bridging organic entity (see Chart 1), lithiation affords a stable nucleophile that can be attacked by electrophiles. The introduction of the thiol functionality (-SH) can be achieved via the reaction with elemental sulfur, in agreement with literature procedures describing the synthesis of organic thiols[45] (see also the Experimental part). Characterization of compound (**3**) was done by nuclear magnetic resonance (NMR) spectroscopy (^1H, ^{13}C, ^{29}Si) and electron-spray ionization mass spectrometry (ESI-MS); data are given in the Supporting Information S-1.

Chart 1. Synthesis Routes Toward the Required PMO Sol−Gel Precursors

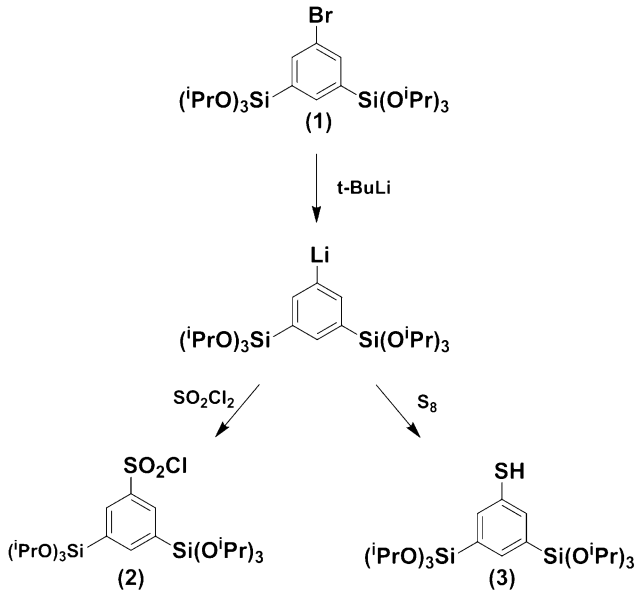

DOI: 10.1021/am5083057
ACS Appl. Mater. Interfaces 2015, 7, 1021−1029

Next, the novel sol–gel precursor (**2**) was used for the preparation of the UKON-2j PMO referring to liquid-crystal templating procedures reported in the literature (see also the Experimental part).[46,47] After removal of the template the resulting mesoporous silica material was characterized by nitrogen physisorption measurements. Figure 1a shows the characteristic isotherm and hysteresis curve of the corresponding mesoporous material with a narrow pore size distribution.

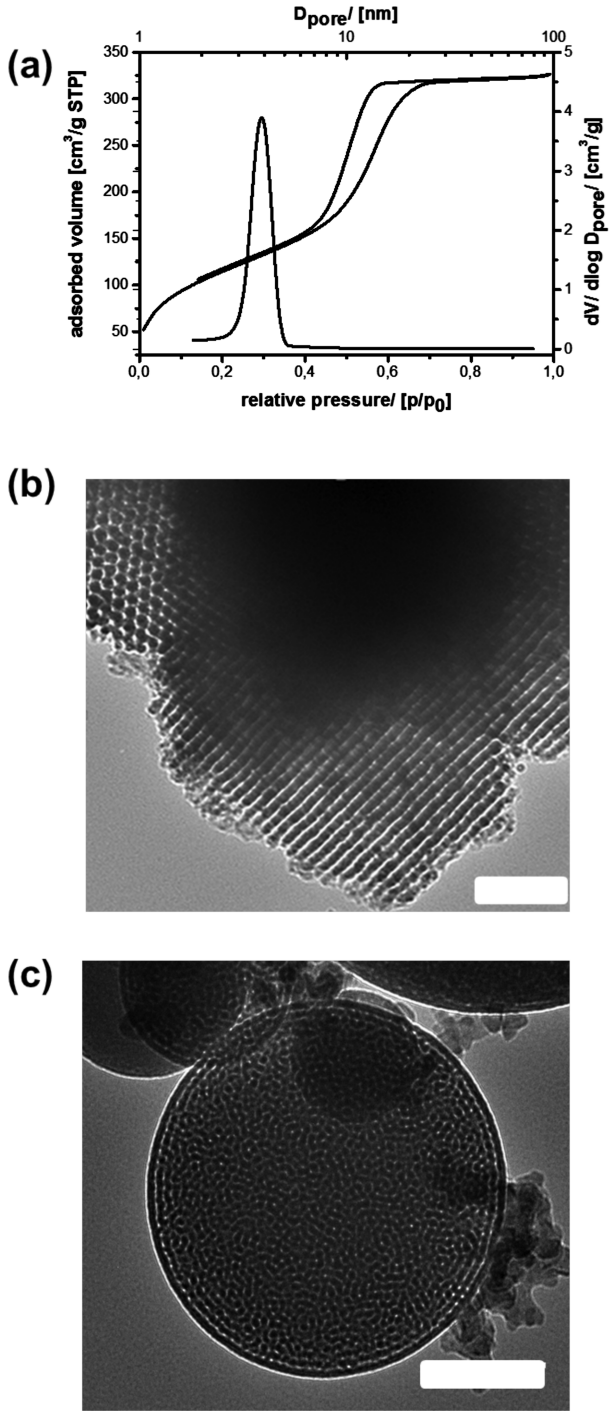

Figure 1. (a) N_2 physisorption data (black) with BJH pore size distribution of UKON-2j (gray). (b) TEM image of hexagonally structured UKON-2j; scale bar = 50 nm. (c) TEM image of UKON-2j nanoparticles prepared via the aerosol-assisted method; scale bar = 100 nm.

According to the Barret/Joyner/Halenda (BJH)[48] evaluation of the isotherm data, the material is characterized by an average pore size of 3.9 nm, and its surface area, calculated using the Brunauer/Emmet/Teller (BET) method, is 450 m^2/g. TEM investigation of UKON-2j demonstrates nicely the high periodic order of the material (Figure 1b). The occurrence of a cylindrical, hexagonally ordered pore system was further secured using small-angle X-ray scattering (SAXS) given in Figure S-2 (SI). The set of scattering signals at q_{10} = 0.56 nm^{-1}, q_{11} = 0.94 nm^{-1}, and q_{20} = 1.12 nm^{-1} is characteristic of the *P6/mm* space group with a periodicity of 11.2 nm. Together with the pore-size determined from N_2 physisorption it can be concluded that the thickness of the pore walls is of the order of 7 nm, which is in good agreement with TEM data (Figure 1b). The chemical nature and composition of UKON-2j was confirmed by a combination of several, independent analytical techniques (see also Figure S-2, SI). The presence of sulfur groups was proven by energy-dispersive X-ray spectroscopy (EDX). The EDX spectrum exhibits a Si:S ratio of 2:1, which precisely corresponds to the value corresponding to the ideal composition $Si_2O_3(C_6H_3SH)$. ^{13}C solid-state NMR is a useful technique by comparing the solid-state NMR signals of UKON-2j directly to the signals received from the precursor (**3**) in solution. The signal characteristic for the carbon atom attached to the sulfur appears in the precursor spectra at a chemical shift of 130 ppm. Consequently the shoulder observed at 129.92 ppm in the NMR spectrum of UKON-2j can be assigned to the thiol group.

The method described so far for the synthesis of mesoporous materials affords powders consisting of ill-defined particles (Figure 1b). For the modification of surfaces one needs much more defined nanoparticles, which may be dispersed in a medium used for evaporation coating methods. Therefore, we transferred a process originally published by Brinker et al. for SiO_2 particles[49] to the UKON-2j system presented here. An aerosol-assisted route was used for generating highly porous PMO nanoparticles in the range of 100 nm–1 μm (see Figure S-3a, SI). A mixture of the prehydrolyzed precursor (**3**), an aqueous HCl/KCl buffer, ethanol, and a structure-directing block copolymer of the pluronic family (see Experimental Section) is evaporated via an aerosol generator. Passing the resulting small droplets of the described sol through a tube oven heated at 400 °C, ethanol evaporates, and increase of the pluronic concentration takes place. This induces the liquid crystal formation. At the same time the condensation of the PMO precursor occurs, and this results in the formation of the mesostructured UKON-2j nanoparticles. The nanoparticles are collected via a filter system and are finally extracted in acidic media. It can be clearly seen from TEM measurements shown in Figure 1c that highly porous, fairly well-structured particles could be obtained. Apart from the difference in the degree in periodic ordering (see also SAXS measurements in Figure S-3g, SI), all other analytical methods (compiled in Figure S-3, SI) indicate that the particulate material is equivalent to UKON-2j.

Preparation of Bifunctional Mesoporous Particles Containing Thiol and Sulfonic Acid Groups. In a previous publication, we were able to show that bifunctional materials containing –NH and –COOH functionalities could be obtained by co-condensation of the two respective PMO-UKON precursors.[38] Because the two functional systems (–SH (**3**), see above; $-SO_3H$ (**2**)[44]) are available now, we have prepared a series of materials (see Table 1) differing in the relative amount of the thiol functionality.

DOI: 10.1021/am5083057
ACS Appl. Mater. Interfaces 2015, 7, 1021–1029

Table 1. Overview for Materials Containing Different Degrees of −SH and $-SO_3H$ Functionalities

sample	SH amount/[%]	surface area/[m^2 g^{-1}]	pore size/[nm]
SH100	100	450	3.9
SH50	50	660	3.9
SO_3H100	0	405	3.5

Due to a significant difference in chemical reactivity of the two precursors, it was realized that a careful control over hydrolysis kinetics (see Figure S-4, SI) is crucial for obtaining well-structured and homogeneous materials with bifunctional character. Therefore, the first step involved the prehydrolysis of two solutions containing the precursors (**2**) and (**3**) separately. A combination of those two solutions was followed by the addition of an ethanolic buffer containing the structure-directing agent. The mixture was then stirred until getting a clear and homogeneous solution. Polycondensation, aging, and template extraction were performed as described before for the monofunctional materials. All materials were investigated using the same set of analytical techniques, and the relevant data are given in Figure S-5 (SI). Successful co-condensation of both precursors can be confirmed using FT-IR spectroscopy by the increase of the dominating O═S vibration band at 1024 cm^{-1} characteristic for aromatic sulfonic acids.[50] Mesoporous organosilica particles with bifunctional character could also be prepared using the aerosol-assisted method, and the relevant data are given in Figure S-5b (SI). The introduction of the sulfonic acid entities clearly shows a significant influence on the structure of PMO materials. The strong ionic character of sulfonic acid groups hinders the formation of a very good structuring, when the neutral block copolymer such as pluronic is used.[44] The degree of structural order decreases by increasing the amount of sulfonic acid entity as seen from TEM and SAXS data. In addition nitrogen physisorption data support the fact that the pore wall thickness as well as the BET surface area decrease with higher percentage of SO_3H entities.

Preparation of Ag-Nanoparticles Inside the Mesoporous, Bifunctional PMO Particles. Next, the potential of the described materials for the adsorption of Ag^+ ions was investigated. The particles were suspended in an aqueous $AgNO_3$ solution and were washed afterward thoroughly with water for removing any nonadsorbed silver ions. The amount of Ag^+ can be compared for different materials using energy-dispersive X-ray spectroscopy (EDX) shown in Figure 2a. The spectra for the materials SH100, SH50, and SO_3H100 are shown after normalization to the intensity of the $Si_{K\alpha}$ peak for better comparison. The SH100 material binds, as expected, a significant amount of Ag^+, indicated by the intense signals for $Ag_{L\alpha,\beta}$. However, it can be seen that also the SO_3H_{100} material leads to a comparable Ag^+ immobilization. For exclusion that surface OH groups are responsible for the interaction with the metal ions,[51] a mesoporous material composed of pure silica was investigated as well. It can be seen that mesoporous silica is not capable of binding Ag^+. After washing the $Ag_{L\alpha,\beta}$ signals are missing. Interestingly, the SH50 material shows the highest capacity for Ag^+ uptake. This fact can be explained by the high BET surface area as well as the large pore diameter compared to SH100 (UKON-2j) and SO_3H100 (UKON-2i). Quantitative evaluation of the EDX data allows us to determine the S:Ag ratio (1:0.8), and this indicates that almost every functional group in SH50 contributes to Ag^+ coordination. Thermogravimetric anaysis (TGA) was applied as an independent technique

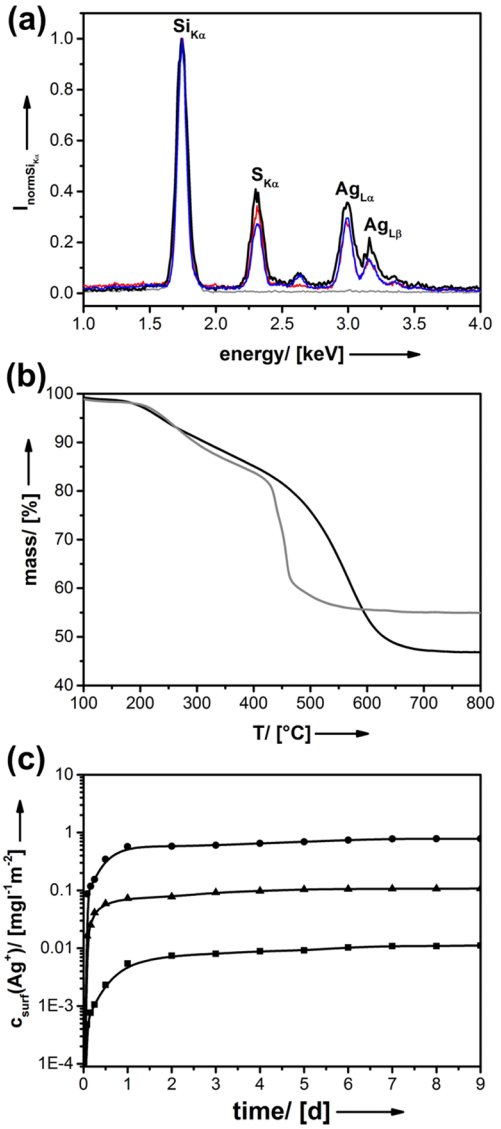

Figure 2. (a) EDX spectra measured after adsorption of Ag^+ in different mesoporous materials. Red graph ≅ SH100; black graph ≅ SH50; blue graph ≅ SO_3H100; gray graph ≅ SiO_2. (b) TGA curves for SH50 (black graph) and Ag^+@SH50 (gray graph). (c) The time dependency of the surface normalized release concentration of silver ions ($c_{surf}(Ag^+)$) obtained via ISE measurements for samples Ag^+@SH100 (squares), Ag^+@SH50 (triangles), and Ag^+@SO_3H100 (circles).

for quantifying the uptake of silver (Figure 2b). Considering SH50 as an exemplary case, two decomposition steps with maxima at 250 and 567 °C can be observed for the starting material. After infiltration of Ag^+ (Ag^+@SH50) the thermal stability of the material has changed. Whereas the position of the first step remains unchanged, the second step is shifted to 455 °C and has become narrower. This points to a potential catalytic role of Ag^+ during the thermal decomposition of UKON materials. Similar observations have been made for SH100 (UKON-2j) and SO_3H100 (UKON-2i) (see Figure S-6 (SI). However, much more direct evidence for the filling of pores with silver comes from the difference in remaining mass at the very end of the thermal decomposition (47% for SH50 and 55% for Ag^+@SH50).

DOI: 10.1021/am5083057
ACS Appl. Mater. Interfaces 2015, 7, 1021−1029

The behavior regarding the release of the loaded silica materials is of pivotal importance for the anticipated biocidal applications. The leaching of Ag^+ from the loaded materials was monitored using a silver ion selective electrode (AgISE) measurement. Because it was already seen that the differing surface area of the materials (see Table 1) has an influence, in order to achieve comparable data, normalization to the specific surface area was done. The results are shown in Figure 2c for three different materials. It can be seen that the equilibrium level of Ag^+ in solution can be controlled via the composition of the (bi)functional organosilica particles. The more thiol groups are present, the lower is the equilibrium concentration of silver ions. After 9 days EDX spectroscopy (shown in Figure S-6, SI) shows that the porous particles are still containing a significant amount of silver, which means that in Figure 2c in fact an equilibrium concentration is shown and not the total release of the metal cations from the pore system. This desired behavior is of course due to the interaction of the functional surface groups with Ag^+.

Next, ascorbic acid was used as a reducing agent for the synthesis of Ag^0 nanoparticles inside the pores of the organosilica materials. Again SH50 is discussed as an exemplary case of a material with bifunctional character. It can be seen from TEM images given in Figure 3a that a large number of nanoparticles with high electronic contrast in the size range 5–10 nm are now present in the SH50 organosilica spheres. Powder X-ray diffraction (given in Figure S-7, SI) proves that these particles are indeed metallic silver. The size of the Ag^0 particles fits perfectly to the range needed for biocidal nanoparticles.[9] Additionally N2-physisorption data (see Figure S-8, SI) of Ag^0@SH50 PMO nanoparticles confirms nicely the presence of porosity with a BET surface area of 340 m^2/g. A potential biocidal application of the shown particles implies that sufficient release of Ag^+ takes place. The mentioned properties were studied again using ISE measurements shown in Figure 3b. Typically, there is a very short induction period of only 2 h, until the Ag^+ reaches a sufficiently high level.

Immobilization of the Resulting Particles on Solid Surfaces. One of the outstanding characteristics of our bifunctional material is the selective use of the thiol functionalities on the outer surface of the particles, which can be used for external modifications. In the current work we apply thiol–ene click chemistry[52,53] for the immobilization of those particles on different surfaces like glass or stainless steel. After fixation of the particle via UV radiation at 365 nm, we tested the stability of the coating by shaking the glass slides for 3 days by 200 rpm in H_2O. Scanning electron microscopy images were taken before and after the washing process and are shown in Figure 4. It can be seen that the particle size distribution is polydisperse, which is typical for particles prepared via aerosol-assisted methods.[54] Nevertheless, the particles have formed a monolayer on the substrate, and the film is fairly dense (Figure 4a). The film features remain unchanged after washing (Figure 4b), which demonstrates the effectiveness of the immobilization method. Comparison to analogous experiments using SO_3H100 or pure SiO_2 particles proves the necessity for the thiol functionalities being in place. As expected, neither SO_3H100 nor SiO_2 particles are capable of the click reaction, and as a consequence they are quantitatively removed from the substrate (see Figure S-9, SI). The mentioned procedure can also be transferred to other surface systems such as stainless steel, which is relevant in marine field (see Figure S-10, SI).

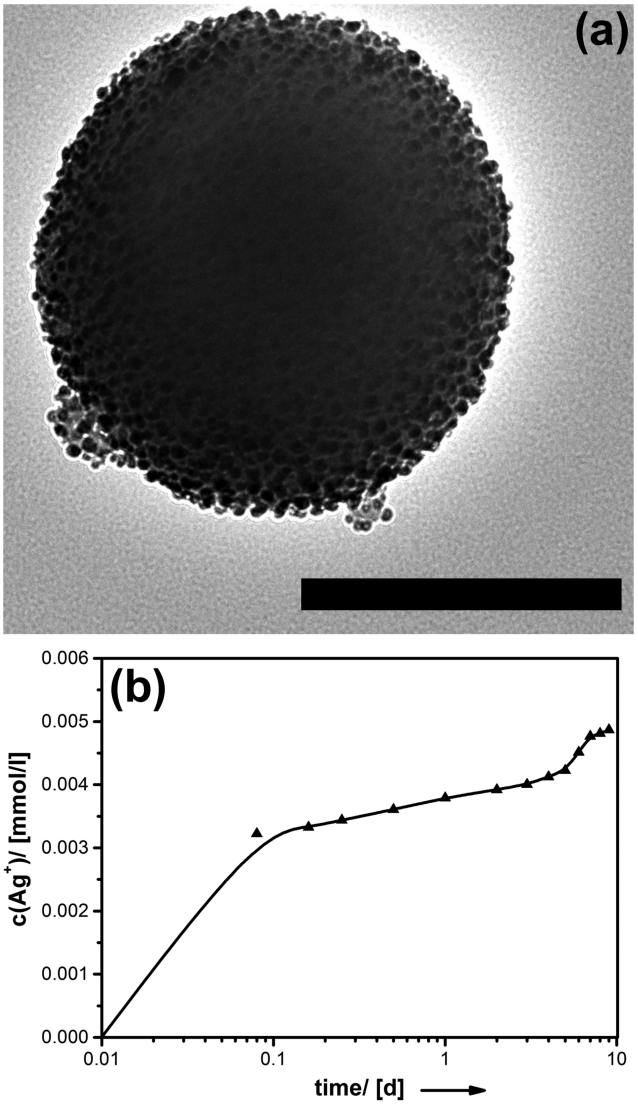

Figure 3. (a) TEM micrograph of one Ag^0@SH50 PMO nanoparticle; scalebar ≅ 200 nm. (b) Ag^+ release from Ag^0SH50 investigated by ISE measurements.

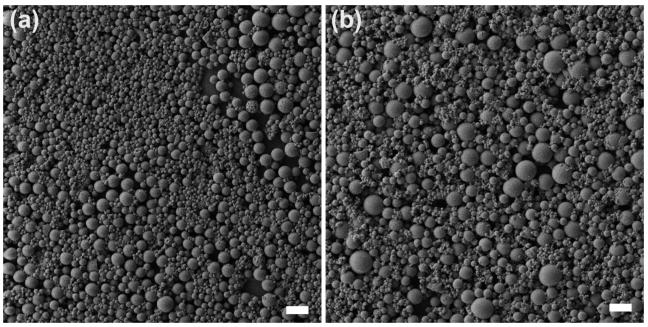

Figure 4. SEM images of mesoporous SH50 particles immobilized on glass substrates via thiol–ene click chemistry before (a) and after washing for 3 days (b). Scalebars ≅ 2 μm.

The procedure established before for the synthesis of Ag^0 nanoparticles inside the mesoporous organosilica hosts was now adopted for the prepared films. TEM measurements show that the loading of SH50 immobilized on glass substrates is successful (as an example, see Figure S-11, SI).

DOI: 10.1021/am5083057
ACS Appl. Mater. Interfaces 2015, 7, 1021–1029

Biological Tests for Antibacterial Activity. First, we checked the properties of the different particles when being freely suspended in bacterial culture fluid (LB medium) and when employing the so-called MIC (minimum inhibitory concentration) test.[55] The MIC is defined as the minimum concentration of a biocidal compound/material that inhibits the growth of, here, a representative biofilm-forming opportunistic pathogen, the bacterium *Pseudomonas aeruginosa* (strain PAO1). The nutrient broth was supplemented with Ag^0@SH50 in different concentrations (0.1−1 mg particles per mL of culture fluid), inoculated with *P. aeruginosa* preculture (1% v/v), incubated for 24 h (shaking), and evaluated for planktonic growth (turbidity) in comparison to untreated controls. The MIC for Ag^0@SH50 was determined at 0.5−0.25 mg/mL (see Figure S-12, SI), which is a very low value for materials based on silver as an antibiocidal agent.[56,57] Importantly, the MIC for Ag^0@SH100 nanoparticles was significantly higher (>1 mg/mL; see Figure S-11, SI), which nicely demonstrates the additional antibacterial influence of the super acidic groups in Ag^0@SH50.

Second, we investigated the effect of the different UKON PMO surface coatings on the viability/survival of attached bacterial cells. Therefore, the surfaces were deliberately "contaminated" with bacteria (*Pseudomonas aeruginosa*) and afterward imprinted on nutrient agar plates (see Figure 5)

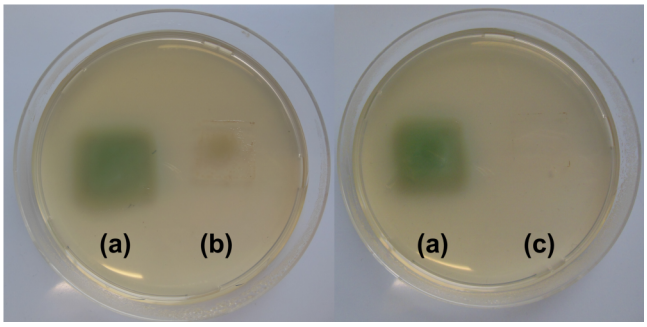

Figure 5. Representative illustration of agar plates that were locally inoculated through imprinting a surface-coated glass slide that had deliberately been "contaminated" with bacteria (*Pseudomonas aeruginosa*), each after 18 h of incubation and in dependence on the surface coating used. The areas of blue-green color indicate undisturbed growth of a dense lawn of *P. aeruginosa* ((a); SiO_2 particles, control), whereas only minor colonization was observed for the imprint of the "contaminated" Ag^0@SH100-coated surface (b), and no growth for the Ag^0@SH50-coated surface (c).

(more details on the experimental procedure are given in the Experimental Section). Pure SiO_2 particles exhibited no biocidal performance (Figure 5a) and were used as a reference. Only minor colonization was observed for the Ag^0@SH100 system (Figure 5b), and complete suppression of bacterial growth was seen for Ag^0@SH50 particles (Figure 5c). The latter observation arguments clearly for a high bacteriocidal activity and large antifouling potential of the materials with bifunctional character ($-SO_3H$ + $-SH$).

Finally, the fate of *P. aeruginosa* cells on the glass slides with and without Ag^0@SH50 mesoporous organosilica particles was investigated by staining and microscopy (Figure 6). Alive and dead bacteria (i.e., bacteria with undisturbed or disturbed membrane integrity, respectively) could be distinguished by staining with "live/dead" stain in combination with fluorescence microscopy. Two effects were observed. First, the overall

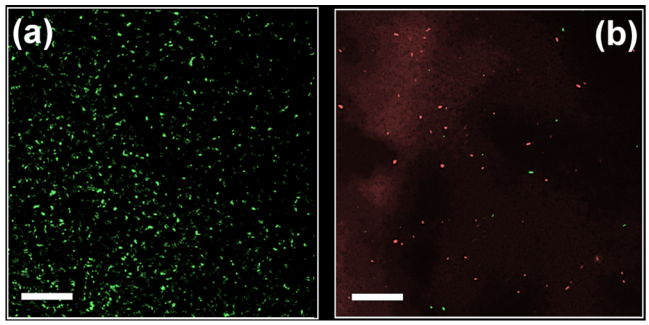

Figure 6. Representative fluorescence microscope images of bacterial cells on bare glass slides (a) and on glass slides coated with Ag^0@SH50 particles (b). Green ≅ live-stained bacterial cells; red ≅ dead-stained bacterial cells. Scale bar = 20 μm.

density of bacteria is much lower for the Ag^0@SH50 coating (Figure 6b) in comparison to the bare glass slide (Figure 6a), which indicates that the bacteria could not attach that well to the particle-coated surface. Second, almost all of the few bacteria on the Ag^0@SH50 film were stained as being dead (Figure 6b).

CONCLUSIONS

The results presented in the current paper can roughly be divided into two parts. First, novel mesoporous organosilica materials with a complex structural and chemical architecture were presented. Then, these materials were developed into effective coatings of glass surfaces and these surfaces tested for their potential as antifouling coating.

A novel periodically ordered mesoporous organosilica material comprising a high density of thiol groups (−SH) could be presented. The availability of the thiol groups enables much more possibilities than presented in the current paper, for instance for the intrapore immobilization of species (e.g., enzymes) via disulfide bridges, to name only one example. The new organosilica material could not only be prepared in the form of conventional powders but also an aerosol-assisted method allowed for the generation of spherical particles with mesoporous substructure in the nano/micrometer range.

A secondary, superacidic function ($-SO_3H$) with additional biocidal activity was introduced by a co-condensation method. Ag^0 nanoparticles were produced inside the pores of the mesoporous particles as an extra level of chemical hierarchy and an additional source for biocidal activity. It could be shown that the presence of the two different functional groups at once is not only beneficial but even mandatory for granting an optimum performance of the materials. The thiol groups are mandatory for the immobilization of the particles on different surfaces like glass or stainless steel and at the same time contribute to the Ag^+ release behavior studied by ion-selective electrodes. Via the amount of sulfonic acid functionality, one can adjust the release of silver ions, and it grants an instantaneous antibacterial activity while the Ag^+ concentration is not yet sufficient. It seems as if the presence of both groups exhibits a cooperative effect in the sense that surfaces protected by these particles are better protected against colonization by bacteria. Furthermore, the presence of both groups seems to optimize the specific surface area and, thus, the accessibility to the functional groups at the pore surfaces.

DOI: 10.1021/am5083057
ACS Appl. Mater. Interfaces 2015, 7, 1021−1029

■ ASSOCIATED CONTENT

Supporting Information

S-1: Characterization of the novel PMO precursor (3) 1,3-bistri(isopropoxysilyl)-thiophenol. S-2: Additional analytical data for the novel PMO material UKON-2j. S-3: Collected analytical data for UKON-2j nanoparticles prepared via the aerosol-assisted route. S-4: Investigation of the prehydrolysis using NMR spectroscopy. S-5: Collected analytical data for bifunctional, mesoporous organosilica materials. S-6: Silver ion Ag^+ loading and release. S-7: PXRD measurement of Ag0@SH50. S-8: N2 physisorption data of Ag0@UKON-SH. S-9: SEM data for immobilization experiments on glass surfaces (reference systems). S-10: SEM/EDX data for immobilization of SH50 particles on stainless steel surfaces. S-11: TEM micrograph of surface-immobilized SH50 nanoparticles loaded with Ag0 nanocrystals. S-12: Biological experiments. This material is available free of charge via the Internet at http://pubs.acs.org.

■ AUTHOR INFORMATION

Corresponding Author

*E-mail: sebastian.polarz@uni-konstanz.de.

Author Contributions

The manuscript was written through contributions of all authors. All authors have given approval to the final version of the manuscript.

Funding

We are highly grateful for funding of the project "Superacidic, porous materials as antibioadhesive coatings' by the Alfred-Kärcher foundation.

Notes

The authors declare no competing financial interest.

■ REFERENCES

(1) Banerjee, I.; Pangule, R. C.; Kane, R. S. Antifouling Coatings: Recent Developments in the Design of Surfaces That Prevent Fouling by Proteins, Bacteria, and Marine Organisms. *Adv. Mater.* **2011**, *23*, 690−718.

(2) Li, Q. L.; Mahendra, S.; Lyon, D. Y.; Brunet, L.; Liga, M. V.; Li, D.; Alvarez, P. J. J. Antimicrobial Nanomaterials for Water Disinfection and Microbial Control: Potential Applications and Implications. *Water Res.* **2008**, *42*, 4591−4602.

(3) Rana, D.; Matsuura, T. Surface Modifications for Antifouling Membranes. *Chem. Rev.* **2010**, *110*, 2448−2471.

(4) Yebra, D. M.; Kiil, S.; Dam-Johansen, K. Antifouling Technology - Past, Present and Future Steps Towards Efficient and Environmentally Friendly Antifouling Coatings. *Prog. Org. Coat.* **2004**, *50*, 75−104.

(5) Feng, Q. L.; Wu, J.; Chen, G. Q.; Cui, F. Z.; Kim, T. N.; Kim, J. O. A Mechanistic Study of the Antibacterial Effect of Silver Ions on Escherichia Coli and Staphylococcus Aureus. *J. Biomed. Mater. Res.* **2000**, *52*, 662−668.

(6) Mijnendonckx, K.; Leys, N.; Mahillon, J.; Silver, S.; Van Houdt, R. Antimicrobial Silver: Uses, Toxicity and Potential for Resistance. *Biometals* **2013**, *26*, 609−621.

(7) Furno, F.; Morley, K. S.; Wong, B.; Sharp, B. L.; Arnold, P. L.; Howdle, S. M.; Bayston, R.; Brown, P. D.; Winship, P. D.; Reid, H. J. Silver Nanoparticles and Polymeric Medical Devices: A New Approach to Prevention of Infection? *J. Antimicrob. Chemother.* **2004**, *54*, 1019−1024.

(8) Yan, Y.; Yang, H.; Li, J.; Lu, X.; Wang, C. Release Behavior of Nano-Silver Textiles in Simulated Perspiration Fluids. *Text. Res. J.* **2012**, *82*, 1422−1429.

(9) Raimondi, F.; Scherer, G. G.; Kotz, R.; Wokaun, A. Nanoparticles in Energy Technology: Examples from Electrochemistry and Catalysis. *Angew. Chem., Int. Ed.* **2005**, *44*, 2190−2209.

(10) Panyala, N. R.; Pena-Mendez, E. M.; Havel, J. Silver or Silver Nanoparticles: A Hazardous Threat to the Environment and Human Health? *J. Appl. Biomed.* **2008**, *6*, 117−129.

(11) Nisola, G. M.; Park, J. S.; Beltran, A. B.; Chung, W.-J. Silver Nanoparticles in a Polyether-Block-Polyamide Copolymer Towards Antimicrobial and Antifouling Membranes. *RSC Adv.* **2012**, *2*, 2439.

(12) Deng, Z.; Zhu, H.; Peng, B.; Chen, H.; Sun, Y.; Gang, X.; Jin, P.; Wang, J. Synthesis of Ps/Ag Nanocomposite Spheres with Catalytic and Antibacterial Activities. *ACS Appl. Mater. Interfaces* **2012**, *4*, 5625−5632.

(13) Zienkiewicz-Strzalka, M.; Pasieczna-Patkowska, S.; Kozak, M.; Pikus, S. Silver Nanoparticles Incorporated onto Ordered Mesoporous Silica from Tollen's Reagent. *Appl. Surf. Sci.* **2013**, *266*, 337−343.

(14) Kim, J. D.; Yun, H.; Kim, G. C.; Lee, C. W.; Choi, H. C. Antibacterial Activity and Reusability of Cnt-Ag and Go-Ag Nanocomposites. *Appl. Surf. Sci.* **2013**, *283*, 227−233.

(15) Agnihotri, S.; Mukherji, S.; Mukherji, S. Immobilized Silver Nanoparticles Enhance Contact Killing and Show Highest Efficacy: Elucidation of the Mechanism of Bactericidal Action of Silver. *Nanoscale* **2013**, *5*, 7328−7340.

(16) Sun, J. M.; Ma, D.; Zhang, H.; Liu, X. M.; Han, X. W.; Bao, X. H.; Weinberg, G.; Pfander, N.; Su, D. S. Toward Monodispersed Silver Nanoparticles with Unusual Thermal Stability. *J. Am. Chem. Soc.* **2006**, *128*, 15756−15764.

(17) Zhu, J.; Konya, Z.; Puntes, V. F.; Kiricsi, I.; Miao, C. X.; Ager, J. W.; Alivisatos, A. P.; Somorjai, G. A. Encapsulation of Metal (Au, Ag, Pt) Nanoparticles into the Mesoporous Sba-15 Structure. *Langmuir* **2003**, *19*, 4396−4401.

(18) Quang, D. V.; Lee, J. E.; Kim, J. K.; Kim, Y. N.; Shao, G. N.; Kim, H. T. A Gentle Method to Graft Thiol-Functional Groups onto Silica Gel for Adsorption of Silver Ions and Immobilization of Silver Nanoparticles. *Powder Technol.* **2013**, *235*, 221−227.

(19) Xue, C.-H.; Chen, J.; Yin, W.; Jia, S.-T.; Ma, J.-Z. Superhydrophobic Conductive Textiles with Antibacterial Property by Coating Fibers with Silver Nanoparticles. *Appl. Surf. Sci.* **2012**, *258*, 2468−2472.

(20) Qin, Y. Q.; Ji, X. H.; Jing, J.; Liu, H.; Wu, H. L.; Yang, W. S. Size Control over Spherical Silver Nanoparticles by Ascorbic Acid Reduction. *Colloids Surf., A* **2010**, *372*, 172−176.

(21) Morones, J. R.; Elechiguerra, J. L.; Camacho, A.; Holt, K.; Kouri, J. B.; Ramirez, J. T.; Yacaman, M. J. The Bactericidal Effect of Silver Nanoparticles. *Nanotechnology* **2005**, *16*, 2346−2353.

(22) White, R. J.; Luque, R.; Budarin, V. L.; Clark, J. H.; Macquarrie, D. J. Supported Metal Nanoparticles on Porous Materials. Methods and Applications. *Chem. Soc. Rev.* **2009**, *38*, 481−494.

(23) Hoffmann, F.; Froba, M. Vitalising Porous Inorganic Silica Networks with Organic Functions-Pmos and Related Hybrid Materials. *Chem. Soc. Rev.* **2011**, *40*, 608−620.

(24) Hoffmann, F.; Cornelius, M.; Morell, J.; Froba, M. Silica-Based Mesoporous Organic-Inorganic Hybrid Materials. *Angew. Chem., Int. Ed.* **2006**, *45*, 3216−3251.

(25) Zhang, S.; Ni, W.; Kou, X.; Yeung, M. H.; Sun, L.; Wang, J.; Yan, C. Formation of Gold and Silver Nanoparticle Arrays and Thin Shells on Mesostructured Silica Nanofibers. *Adv. Funct. Mater.* **2007**, *17*, 3258−3266.

(26) Hoffmann, F.; Cornelius, M.; Morell, J.; Froba, M. Silica-Based Mesoporous Organic-Inorganic Hybrid Materials. *Angew. Chem., Int. Ed.* **2006**, *45*, 3216−3251.

(27) Peng, J.; Yao, Y.; Zhang, X.; Li, C.; Yang, Q. Superhydrophobic Mesoporous Silica Nanospheres Achieved Via a High Level of Organo-Functionalization. *Chem. Commun.* **2014**, *50*, 10830−10833.

(28) Sanchez, C.; Julian, B.; Belleville, P.; Popall, M. Applications of Hybrid Organic-Inorganic Nanocomposites. *J. Mater. Chem.* **2005**, *15*, 3559−3592.

(29) Inagaki, S.; Guan, S.; Fukushima, Y.; Ohsuna, T.; Terasaki, O. Novel Mesoporous Materials with a Uniform Distribution of Organic

DOI: 10.1021/am5083057
ACS Appl. Mater. Interfaces 2015, 7, 1021−1029

Groups and Inorganic Oxide in Their Frameworks. *J. Am. Chem. Soc.* **1999**, *121*, 9611−9614.
(30) Melde, B. J.; Holland, B. T.; Blanford, C. F.; Stein, A. Mesoporous Sieves with Unified Hybrid Inorganic/Organic Frameworks. *Chem. Mater.* **1999**, *11*, 3302−3308.
(31) Asefa, T.; MacLachlan, M. J.; Coombs, N.; Ozin, G. A. Periodic Mesoporous Organosilicas with Organic Groups inside the Channel Walls. *Nature* **1999**, *402*, 867−871.
(32) Esquivel, D.; van den Berg, O.; Romero-Salguero, F. J.; Du Prez, F.; Van Der Voort, P. 100% Thiol-Functionalized Ethylene Pmos Prepared by ″Thiol Acid-Ene″ Chemistry. *Chem. Commun.* **2013**, *49*, 2344−2346.
(33) Hatton, B.; Landskron, K.; Whitnall, W.; Perovic, D.; Ozin, G. A. Past, Present, and Future of Periodic Mesoporous Organosilicas - the Pmos. *Acc. Chem. Res.* **2005**, *38*, 305−312.
(34) Wang, W. D.; Lofgreen, J. E.; Ozin, G. A. Why Pmo? Towards Functionality and Utility of Periodic Mesoporous Organosilicas. *Small* **2010**, *6*, 2634−2642.
(35) Van der Voort, P.; Esquivel, D.; De Canck, E.; Goethals, F.; Van Driessche, I.; Romero-Salguero, F. J. Periodic Mesoporous Organosilicas: From Simple to Complex Bridges; a Comprehensive Overview of Functions, Morphologies and Applications. *Chem. Soc. Rev.* **2013**, *42*, 3913−3955.
(36) Kuschel, A.; Sievers, H.; Polarz, S. Amino Acid Silica Hybrid Materials with Mesoporous Structure and Enantiopure Surfaces. *Angew. Chem., Int. Ed.* **2008**, *47*, 9513−9517.
(37) Polarz, S.; Kuschel, A. Chemistry in Confining Reaction Fields with Special Emphasis on Nanoporous Materials. *Chem.−Eur. J.* **2008**, *14*, 9816−9829.
(38) Kuschel, A.; Drescher, M.; Kuschel, T.; Polarz, S. Bifunctional Mesoporous Organosilica Materials and Their Application in Catalysis: Cooperative Effects or Not? *Chem. Mater.* **2010**, *22*, 1472−1482.
(39) Kuschel, A.; Luka, M.; Wessig, M.; Drescher, M.; Fonin, M.; Kiliani, G.; Polarz, S. Organic Ligands Made Porous: Magnetic and Catalytic Properties of Transition Metals Coordinated to the Surfaces of Mesoporous Organosilica. *Adv. Funct. Mater.* **2010**, *20*, 1133−1143.
(40) Kuschel, A.; Polarz, S. Effects of Primary and Secondary Surface Groups in Enantioselective Catalysis Using Nanoporous Materials with Chiral Walls. *J. Am. Chem. Soc.* **2010**, *132*, 6558−6565.
(41) Mascotto, S.; Wallacher, D.; Kuschel, A.; Polarz, S.; Zickler, G. A.; Timmann, A.; Smarsly, B. M. Adsorption in Periodically Ordered Mesoporous Organosilica Materials Studied by in Situ Small-Angle X-Ray Scattering and Small-Angle Neutron Scattering. *Langmuir* **2010**, *26*, 6583−6592.
(42) Luka, M.; Polarz, S. Stimuli-Responsive Mesoporous Organosilica Materials Containing Ph-Sensitive Organic Dyes. *Microporous Mesoporous Mater.* **2013**, *171*, 35−43.
(43) Wessig, M.; Drescher, M.; Polarz, S. Probing Functional Group Specific Surface Interactions in Porous Solids Using Esr Spectroscopy as a Sensitive and Quantitative Tool. *J. Phys. Chem. C* **2013**, *117*, 2805−2816.
(44) Gehring, J.; Schleheck, D.; Luka, M.; Polarz, S. Aerosol-Synthesis of Mesoporous Organosilica Nanoparticles with Highly Reactive, Superacidic Surfaces Comprising Sulfonic Acid Entities. *Adv. Funct. Mater.* **2014**, *24*, 1140−1150.
(45) Jones, E.; Moodie, I. M. 2-Thiophenethiol. *Org. Synth.* **1988**, *50−9*, 979−980.
(46) Morell, J.; Wolter, G.; Froba, M. Synthesis and Characterization of Highly Ordered Thiophene-Bridged Periodic Mesoporous Organosilicas with Large Pores. *Chem. Mater.* **2005**, *17*, 804−808.
(47) Morell, J.; Gungerich, M.; Wolter, G.; Jiao, J.; Hunger, M.; Klar, P. J.; Froba, M. Synthesis and Characterization of Highly Ordered Bifunctional Aromatic Periodic Mesoporous Organosilicas with Different Pore Sizes. *J. Mater. Chem.* **2006**, *16*, 2809−2818.
(48) Barrett, E. P.; Joyner, L. G.; Halenda, P. P. The Determination of Pore Volume and Area Distributions in Porous Substances 0.1. Computations from Nitrogen Isotherms. *J. Am. Chem. Soc.* **1951**, *73*, 373−380.
(49) Lu, Y.; Fan, H.; Stump, A.; Ward, T. L.; Rieker, T.; Brinker, C. J. Aerosol-Assisted Self-Assembly of Mesostructured Spherical Nanoparticles. *Nature* **1999**, *398*, 223−226.
(50) Hakki, A.; Dillert, R.; Bahnemann, D. W. Arenesulfonic Acid-Functionalized Mesoporous Silica Decorated with Titania: A Heterogeneous Catalyst for the One-Pot Photocatalytic Synthesis of Quinolines from Nitroaromatic Compounds and Alcohols. *ACS Catal.* **2013**, *3*, 565−572.
(51) Bronstein, L. M.; Polarz, S.; Smarsly, B.; Antonietti, M. Sub-Nanometer Noble-Metal Particle Host Synthesis in Porous Silica Monoliths. *Adv. Mater.* **2001**, *13*, 1333−1336.
(52) Hoyle, C. E.; Bowman, C. N. Thiol-Ene Click Chemistry. *Angew. Chem., Int. Ed.* **2010**, *49*, 1540−1573.
(53) Lowe, A. B. Thiol-Ene ″Click″ Reactions and Recent Applications in Polymer and Materials Synthesis. *Polym. Chem.* **2010**, *1*, 17−36.
(54) Swihart, M. T. Vapor-Phase Synthesis of Nanoparticles. *Curr. Opin. Colloid Interface Sci.* **2003**, *8*, 127−133.
(55) Murray, B. E. The Life and Times of the Enterococcus. *Clin. Microbiol. Rev.* **1990**, *3*, 46−65.
(56) Guzman, M.; Dille, J.; Godet, S. Synthesis and Antibacterial Activity of Silver Nanoparticles against Gram-Positive and Gram-Negative Bacteria. *Nanomed.-Nanotechnol. Biol. Med.* **2012**, *8*, 37−45.
(57) Weir, E.; Lawlor, A.; Whelan, A.; Regan, F. The Use of Nanoparticles in Anti-Microbial Materials and Their Characterization. *Analyst* **2008**, *133*, 835−845.

DOI: 10.1021/am5083057
ACS Appl. Mater. Interfaces 2015, 7, 1021−1029